Chinese Chemical Letters 31 (2020) 2960–2964

Contents lists available at ScienceDirect

Chinese Chemical Letters

journal homepage: www.elsevier.com/locate/cclet

Communication

Development of BINOL-Si complexes with large stokes shifts and their application as chemodosimeters for nerve agent

Xu Feng[a], Yawen Wang[b,**], Wenlin Feng[c], Yu Peng[a,b,*]

[a] State Key Laboratory of Applied Organic Chemistry, Lanzhou University, Lanzhou 730000, China
[b] School of Life Science and Engineering, Southwest Jiaotong University, Chengdu 610031, China
[c] Department of Physics and Energy, Chongqing University of Technology, Chongqing 400054, China

ARTICLE INFO

Article history:
Received 9 March 2020
Received in revised form 27 May 2020
Accepted 30 May 2020
Available online 1 June 2020

Keywords:
Nerve agent
BINOL derivatives
Si complex
Fluorescent probe
DCP

ABSTRACT

Three fluorescent BINOL-Si complexes (FS1, FS2 and FS3) were rationally designed and synthesized to detect diethyl chlorophosphate (DCP), a mimic of lethal nerve agents. These three fluorescent probes showed green, yellow and orange fluorescence, respectively. Moreover, the series of fluorescent probes has the characteristics of fast response time ($\leq$ 4 s), low detection limit (0.0097 μmol/L), high sensitivity and naked eye detection. More important, a fiber optic sensor capable of detecting DCP vapor in real time was also prepared for the first time, the lowest detection limits (down to 4.4 ppb) were all lower than that of the IDLH (immediately dangerous to life or health) concentration of Sarin (7.0 ppb).

The 1,1′-binaphthol (BINOL) is a polycyclic compound with the unique rigid conformation, which emits fluorescence at about 375 nm for monomer and 440 nm for excimer when excited at 340 nm [1–3] Its derivatives have been widely used in molecular recognition [4–8]. Silicon belongs to the third cycle of the periodic table and is the common element of the IVA family. In the past decade, silicon-containing compounds have been widely used in various fields [9–16]. However, small molecules containing silicon with long-wavelength fluorescence only exist in rhodamine and coumarin derivatives at present [17–23]. Adding silicon to the skeleton of BINOL can make it become a new class of fluorescent probe with longer wavelength emission, and therefore provide an alternative fluorescent material for the recognition.

Due to their high toxicity, organophosphorus compounds (OPS) are widely used as pesticides and herbicides in agriculture [24]. But they are even utilized as chemical warfare agents (CWAs) in the war. Among them, a series of phosphoric acid esters are discovered as nerve agents. They can cause irreversible damage to acetyl cholinesterase in the human nervous system and affect nerve transmission. As a result, people exposed to nerve agents eventually would die of respiratory paralysis [25,26]. G-type nerve agents (Fig. 1a), including Tabun (GA), Sarin (GB), Soman (GD) and Cyclosarin (GF), appeared during the Second World War. Although such CWAs are strictly restricted in the international community, there are still incidents in which terrorists use them to take people's life, such as the horrible attack in Tokyo subway. Thus, rapid detection of these nerve agents in convenient way is essential for public security system.

In recent years, some nanofibers [27–29] and organic small molecules [30–38] as fluorescent probes have been developed for the detection of mimics of nerve agents due to their easy preparation, high sensitivity and fast response. In comparison with other analytes [39–41], the reported fluorescent probes for nerve agents were still scarce. More importantly, most of these probes are lack of practical applications and precise detection [42–46]. Therefore, development of fluorescent probes with higher sensitivity and real-time monitoring are highly desirable.

In connection with our continuing study to probes with 1,1′-binaphthyl scaffold [47–52], herein we synthesized three Si-containing probes based on this unique structure for the first time (Fig. 1b). Moreover, these probes can be used to detect DCP [53] with high sensitivity and specificity through a chemical reaction. Compared with FP compounds, the Si-containing probes (FS1, FS2 and FS3) have stronger fluorescence (Fig. S1 in Supporting information). Notably, compared with other fluorescent probes (Table S1 in Supporting information) [54–58], FS1, FS2 and FS3 have larger Stokes shifts (up to 244 nm) and the maximum fluorescence emissions shift to longer wavelengths (up to 582 nm for monomer). In addition, FS1 and FS2 respond to DCP in less than

* Corresponding author at: State Key Laboratory of Applied Organic Chemistry, Lanzhou University, Lanzhou 730000, China.
** Corresponding author.
E-mail addresses: ywwang@swjtu.edu.cn (Y. Wang), pengyu@lzu.edu.cn (Y. Peng).

https://doi.org/10.1016/j.cclet.2020.05.042
1001-8417/

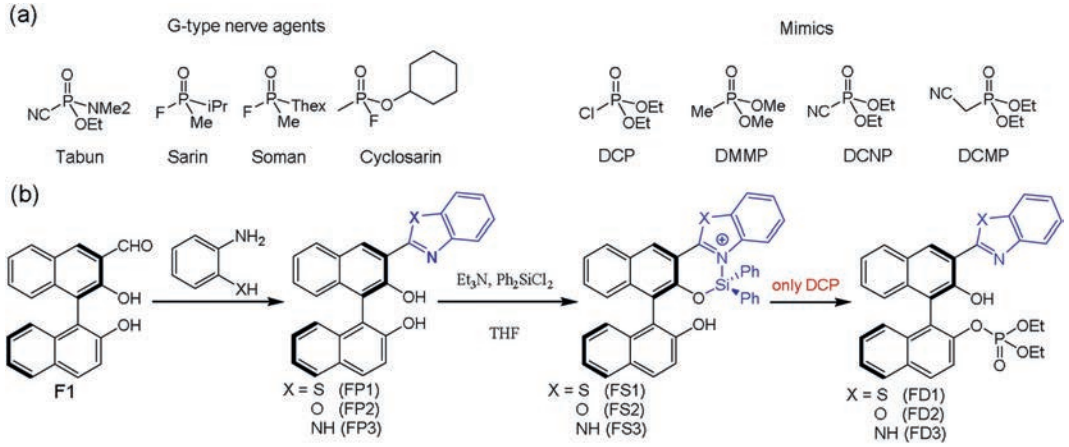

Fig. 1. (a) The structures of G-type nerve agents and the mimics of nerve agents. (b) The synthesis of fluorescent probes (FS1, FS2 and FS3) and reaction products with DCP, respectively.

4 s, faster than most other fluorescent probe molecules. The real-time accurate detection of DCP has also been achieved by using fiber-optic sensing technology for the first time [59].

Designed probes FS1, FS2 and FS3 were obtained by the Ph_2SiCl_2 with corresponding ligands (detailed experimental procedures and Figs. S2-S10 in Supporting information). Their structures were confirmed by ^{1}H, ^{13}C NMR, IR and mass spectra (Figs. S11-S19 in Supporting information). Firstly, the photophysical properties of FS1, FS2 and FS3 were studied in DMF solution at room temperature (Fig. 2). In the UV–vis spectrum, the maximum absorption peaks of FS1, FS2 and FS3 were 338, 321 and 339 nm, respectively. Upon excitation by the corresponding absorption lights, FS1, FS2 and FS3 showed strong fluorescence at about 582, 531 and 516 nm, respectively. The relatively large Stokes shifts were also obtained (FS1: 244 nm; FS2: 210 nm; FS3: 177 nm). And for FS3, an excimer emission peak at about 600 nm was also observed, which increased with enhancement of the concentration (Fig. S20 in Supporting information). Accordingly, the fluorescence colors included green, yellow and orange (Fig. 2, inset), which showed that the fluorescence of BINOL-Si was tunable and potential to obtain full-color wavelength materials.

To better understand the above photophysical properties, TDDFT calculations with B3LYP/6−31G basis set were carried out using the Gaussian 09 program (Fig. 3 and Figs. S21−S23 in Supporting information). For all of probes, the main contribution transition was HOMO–3 to LUMO. The electron density of their HOMO–3 orbitals was mainly distributed in one naphthalene ring of probes. In contrast, the LUMO of probes was located at the section of silicon complex in probes, which indicated the strong fluorescence character. These results were in good agreement with the fluorescence spectra of probes.

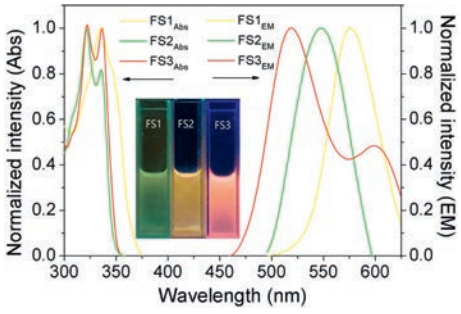

Fig. 2. Normalized absorption and emission spectra of FS1, FS2 and FS3 (10.0 μmol/L) in DMF. Inset: Pictures of FS1, FS2 and FS3 in DMF under UV light at 365 nm.

FS1, FS2 and FS3 were then used to detect DCP. As shown in Fig. 4c, some mimics of nerve agents such as dimethyl methyl phosphate (DMMP), diethyl cyanophosphonate (DCNP), and diethyl cyanomethylphosphonate (DCMP) hardly had any influence on the fluorescence of probes. Only DCP generated significant fluorescence changes. The fluorescence color also changed from yellow to blue for FS1, from green to dark green for FS2, and from orange to red for FS3, all of which could be observed clearly by the naked eye. These results indicated that FS1, FS2 and FS3 had excellent selectivity for DCP. The fluorescence titrations were next conducted (Fig. 4d, Figs. S24 and S25 in Supporting information). With the addition of DCP to the solution of FS1, remarkable decreases in fluorescence intensity occurred at 582 nm and a new peak at 475 nm appeared. A good linear relationship of the emission intensity ratios (F_{582}/F_{475}) were achieved with increasing DCP concentration from 1.0 μmol/L to 10.0 μmol/L (Fig. 4d, inset), which indicated that FS1 can be used as a ratiometric fluorescence probe for DCP. For FS2, the fluorescence at 531 nm quenched gradually (Fig. S24 in Supporting information). After the addition of DCP to the solution of FS3 (Fig. S25 in Supporting information), the emission band centered at 516 nm decreased obviously. The peak at about 600 nm almost did not decrease, since the excimer emission of the corresponding product appeared just there (Fig. S26 in Supporting information). These changes in fluorescence spectra were all in good agreement with the changes of fluorescence color.

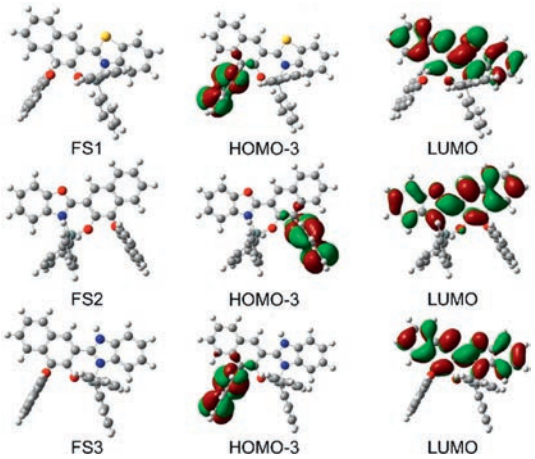

Fig. 3. The optimized structures and molecular orbital plots of FS1, FS2 and FS3.

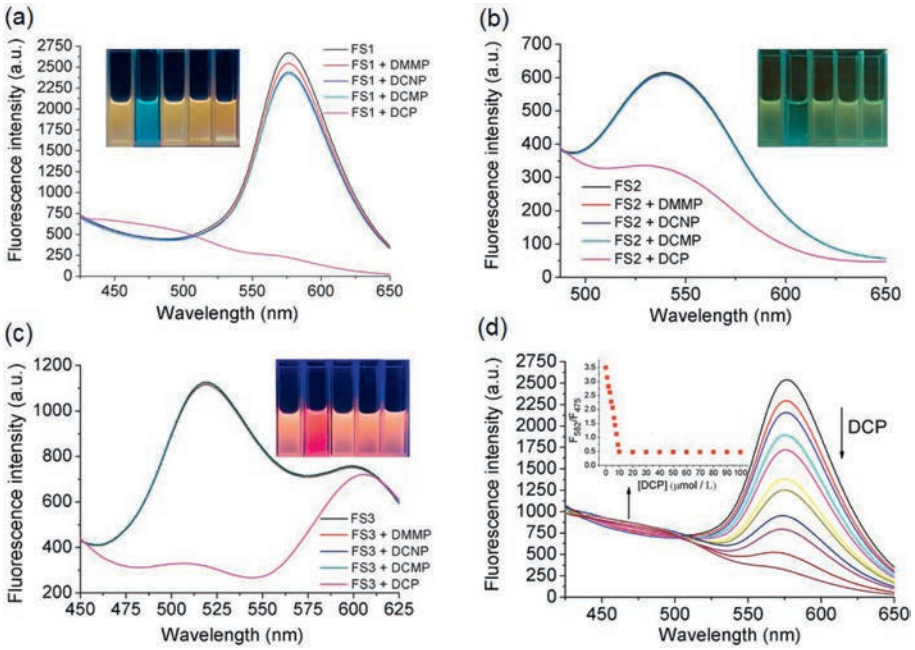

Fig. 4. (a-c) Fluorescence spectra of FS1, FS2 and FS3 (10.0 μmol/L) upon the addition of different mimics (DMMP, DCNP, DCMP and DCP) (DMF, [mimics] = 10.0 μmol/L) (FS1: λ_{ex} = 338 nm, FS2: λ_{ex} = 321 nm, FS3: λ_{ex} = 339 nm). Inset: Pictures of FS1, FS2 and FS3 with mimics (from left to right: none, DCP, DMMP, DCNP and DCMP). (d) Fluorescence spectra changes of FS1 (10.0 μmol/L) toward DCP (0.0, 1.0, 2.0, 3.0, 4.0, 5.0, 6.0, 7.0, 8.0, 9.0, 10.0, 20.0, 30.0, 40.0, 50.0, 60.0, 70.0, 80.0, 90.0 and 100.0 μmol/L). Inset: Fluorescence intensity at F_{582}/F_{475} changes upon the addition of DCP.

Subsequently, the detection limits [60] of FS1, FS2 and FS3 were calculated to be 0.17, 0.0097 and 0.11 μmol/L for DCP, respectively (Fig. S27 in Supporting information). Fluorescence quantum yield [61] of FS1, FS2 and FS3 decreased from 3.86% to 0.82%, 1.25% to 0.51%, and 1.89% to 0.93%, respectively, in the presence of DCP (1.0 equiv.). For FS1 or FS2, the fluorescence intensity at 582 nm or 531 nm weakened to the minimum value within less than 4 s as soon as DCP was added. Thus, the kinetic constant of FS1 or FS2 toward DCP cannot be obtained (Fig. S28 in Supporting information). The observed rate constant (k_{obs}) of FS3 was calculated to be 4.47×10^{-2} min^{-1} by fitting the fluorescence intensity changes [62]. These results indicated that these probes can provide very rapid and sensitive responses to DCP.

To verify the detection mechanism, ^{1}H NMR titration experiments were performed (Fig. 5 and Figs. S29–S30 in Supporting information). As shown in Fig. 5, H_1 and H_2 (Fig. 5a) are the proton signals of the hydroxyl and amino group of FS3, respectively. Upon the addition of DCP to the solution, the signal of H_1 weakened (Fig. 5b), then disappeared (Fig. 5c). And the signal of H_2 had almost no change. These results suggested that the hydroxyl group (−OH_1) of FS3 reacted with DCP to form a P−O bond. However, a new signal appeared at 13.46 ppm, which indicated that the silicon complex decomposed. To confirm the product of FS3 and DCP, a preparative experiment was carried out (Supporting information). FD3 was thus obtained, and the signal of 13.46 ppm could be attributed to H_3 in FD3. The similar changes were also observed in the case of FS1 (Fig. S29) or FS2 (Fig. S30). All of FD1, FD2, and FD3 were characterized by ^{1}H, ^{13}C NMR spectroscopy, MS and X-ray diffraction analysis [63] (Figs. S31–S40 and Table S2 in Supporting information). When a large excess of DCP was added (Fig. 5d), the spectrum obtained was almost the same as that of Fig. 5c. These results suggested that DCP react with the OH_1 group in FS compounds firstly. The Si moiety then decomposed by HCl generated *in situ*. But only phenol products (FD1, FD2 and FD3) were obtained. Notably, the single-crystal X-ray diffraction analysis revealed that there were intramolecular H-bonds in FD1, FD2 and FD3 (Fig. S41 in Supporting information). The N–O distances were 2.622, 2.650 and 2.613 Å for FD1, FD2 and FD3, respectively. And the corresponding O-H . . . N angles were

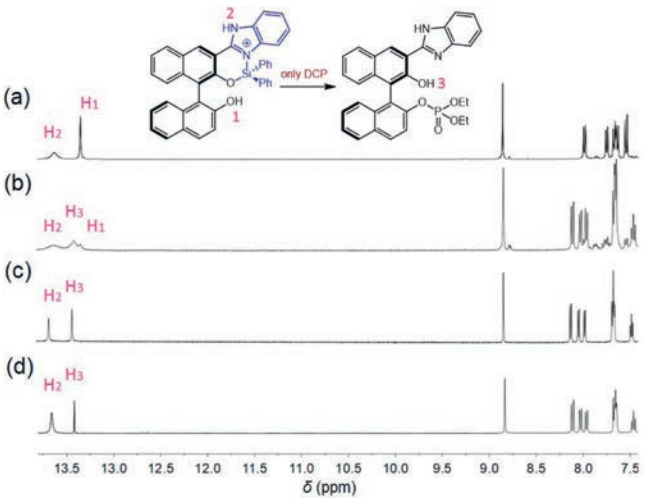

Fig. 5. Partial ^{1}H NMR spectra of FS3 with DCP (DMSO-d_6, 400 MHz). (a) FS3 only, (b) FS3 + DCP (0.5 equiv.), (c) FS3 + DCP (1.0 equiv.), (d) FS3 + DCP (10.0 equiv.).

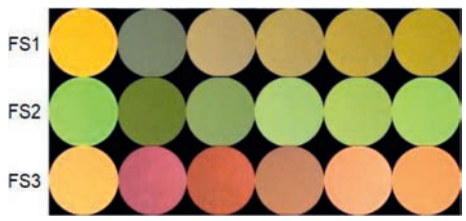

Fig. 6. The color changes of paper sensors for the visual detection of DCP with different concentrations under UV light. From left to right: [DCP] = 0, 10.0, 5.0, 2.5, 1.0 and 0.5 mmol/L.

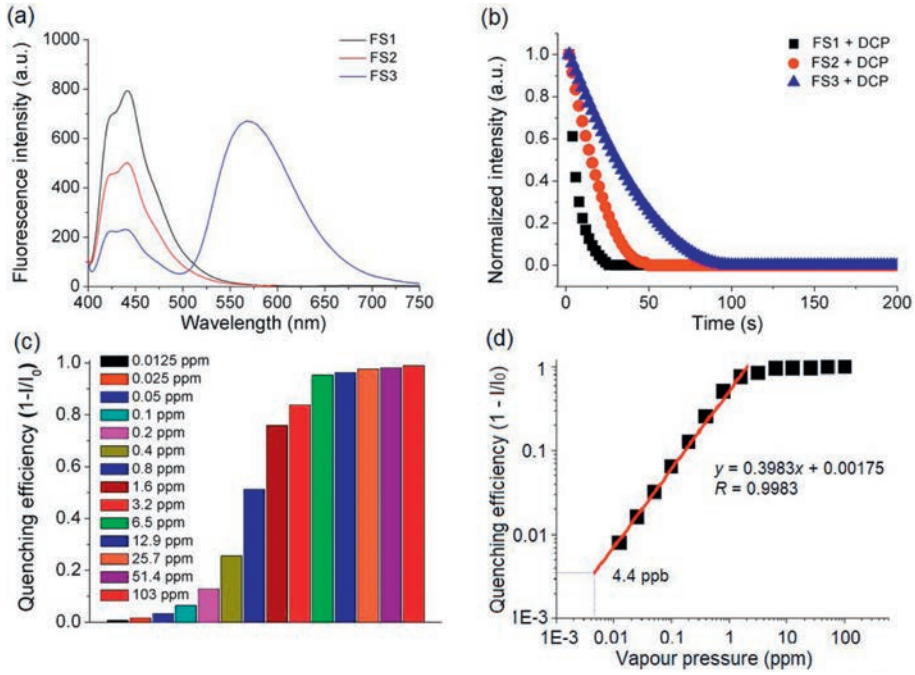

Fig. 7. (a) Fluorescence spectra of FS1, FS2 and FS3. (b) The time responses of FS1, FS2 and FS3 with DCP vapor. (c) The quenching efficiency of FS2 after exposure to different concentrations of DCP vapor for 100 s. (d) The linear fitting function of fluorescence quenching rate of FS2.

148.79°, 148.88° and 145.16° for FD1, FD2 and FD3, respectively. Especially, there was an intermolecular H-bond in compound FD3 between –NH of imidazole group and the oxygen atom in P=O of another FD3 molecule. The corresponding N–O distance and O-H . . . N angle were 2.842 Å and 165.93° respectively. These results indicated that the existence of hydrogen bonds was the plausible reason for selective formation of FD1, FD2 and FD3.

Filter papers, which were first immersed in the solutions containing probes (10.0 mmol/L), had been used to make paper sensors to detect DCP. As shown in Fig. 6, these paper sensors exhibited yellow color for FS1, green color for FS2, and orange color for FS3, respectively. With the increase of DCP, fluorescence quenching (FS1 and FS2) or color changes (FS3) were clearly observed by the naked eye.

Optical fiber sensing technology is a new type of sensing technology with broad prospects. Its advantages include anti-electromagnetic interference, small energy loss and high accuracy. A device of fiber optic sensor was also fabricated by combining these probes with fiber sensing technology (Figs. S42 and S43 in Supporting information) for the detection of DCP vapor. Fluorescent probe (10.0 μmol/L) was dissolved in acetone (1.0 L) and was coated on the surface of the fiber optic probe. After sufficiently drying, a film was formed as a sensing element. The fluorescence spectra of FS1, FS2 and FS3 (Fig. 7a) were obtained at 380 nm excitation. The response times of FS1, FS2 and FS3 for DCP vapor were about 20, 45 and 90 s, respectively (Fig. 7b). In order to obtain the detection limit, the quenching efficiency of FS1, FS2 and FS3 *versus* different concentrations of DCP vapor (0.0125, 0.025, 0.05, 0.1, 0.2, 0.4, 0.8, 1.6, 3.2, 6.5, 12.9, 25.7, 51.4 and 103 ppm) were monitored (Fig. 7c and Fig. S44 in Supporting information). According to the fluorescence quenching rate, the corresponding detection limits of FS1, FS2 and FS3 were 6.6, 4.4 and 6.8 ppb, respectively (Fig. 7d and Fig. S45 in Supporting information), which were all lower than that of the IDLH (immediately dangerous to life or health) concentration of Sarin (7.0 ppb) [54]. These results showed that the fiber sensors could achieve low concentration detection and short response time for DCP vapor.

In summary, new fluorescent probes FS1–FS3 were successfully designed to tune the emission character of BINOL fluorophore, with up to 244 nm Stokes shift. They showed fast, sensitive and specific response to dangerous DCP as a threat to public security. Furthermore, the rapid detection of DCP vapor could be achieved in fiber optic sensor with high precision and sensitivity.

Declaration of competing interest

The authors declare that they have no known competing financial interests or personal relationships that could have appeared to influence the work reported in this paper.

Acknowledgments

This work was supported by the National Natural Science Foundation of China (Nos. 21572091 and 21772078), the Fundamental Research Funds for the Central Universities (Nos. 2682019CX70 and 2682019CX71).

Appendix A. Supplementary data

Supplementary material related to this article can be found, in the online version, at doi:https://doi.org/10.1016/j.cclet.2020.05.042.

References

[1] V.P. Muralidharan, K.I. Sathiyanarayanan, ChemistrySelect 3 (2018) 3111–3117.
[2] Z.B. Li, J. Lin, L. Pu, Angew. Chem. Int. Ed. 44 (2005) 1690–1693.
[3] Z.B. Li, J. Lin, M. Sabat, M. Hyacinth, L. Pu, J. Org. Chem. 72 (2007) 4905–4916.
[4] L. Pu, Acc. Chem. Res. 45 (2011) 150–163.
[5] F. Zhao, Y. Du, J. Tian, et al., Eur. J. Org. Chem. 16 (2018) 1891–1895.
[6] A.S. Gupta, G. Kumar, K. Paul, V. Luxami, New J. Chem. 42 (2018) 2491–2497.
[7] K. Wen, S. Yu, Z. Huang, et al., J. Am. Chem. Soc. 137 (2015) 4517–4524.
[8] T. Hashimoto, Y. Naganawa, K. Maruoka, J. Am. Chem. Soc. 133 (2011) 8834–8837.
[9] Y. Koide, Y. Urano, K. Hanaoka, T. Terai, T. Nagano, J. Am. Chem. Soc. 133 (2011) 5680–5682.
[10] T. Wang, Q.J. Zhao, H.G. Hu, et al., Chem. Commun. 48 (2012) 8781–8783.
[11] G. Lukinavičius, K. Umezawa, N. Olivier, et al., Nat. Chem. 5 (2013) 132–139.

[12] H. Wang, H. Xie, Y. Liang, et al., J. Mater. Chem. C 1 (2013) 5367–5372.
[13] J. Miao, Y. Huo, H. Shi, et al., J. Mater. Chem. B 6 (2018) 4466–4473.
[14] J.B. Grimm, T. Klein, B.G. Kopek, et al., Angew. Chem. Int. Ed. 55 (2016) 1723–1727.
[15] T. Song, Z.S. Li, J.G. Liu, S.Y. Yang, Chin. Chem. Lett. 23 (2012) 793–796.
[16] A.L. Li, Y.P. Ma, D. Qiu, Chin. Chem. Lett. 26 (2015) 152–156.
[17] C. Li, T. Wang, N. Li, et al., Chem. Commun. 55 (2019) 11802–11805.
[18] X. Zhang, J. Wang, P. Wang, et al., Chem. Commun. 55 (2019) 10916–10919.
[19] M. Du, B. Huo, J. Liu, et al., J. Mater. Chem. C 6 (2018) 10472–10479.
[20] J. Tang, Q. Li, Z. Guo, W. Zhu, Org. Biomol. Chem. 17 (2019) 1875–1880.
[21] K. Hanaoka, Y. Kagami, W. Piao, et al., Chem. Commun. 54 (2018) 6939–6942.
[22] Y. Huo, J. Miao, L. Han, et al., Chem. Sci. 8 (2017) 6857–6864.
[23] M. Fu, Y. Xiao, X. Qian, D. Zhao, Y. Xu, Chem. Commun. 15 (2008) 1780–1782.
[24] I. Walton, M. Davis, L. Munro, et al., Org. Lett. 14 (2012) 2686–2689.
[25] S. Royo, R. Martínez-Máñez, F. Sancenón, et al., Chem. Commun. 46 (2007) 4839–4847.
[26] J. Bajgar, Adv. Clin. Chem. 38 (2004) 151–216.
[27] L. Chen, H. Oh, D. Wu, M.H. Kim, J. Yoon, Chem. Commun. 54 (2018) 2276–2279.
[28] J. Lee, E. Seo, M. Yoo, et al., Polymer 179 (2019)121664.
[29] K.T. Alali, J. Liu, K. Aljebawi, et al., J. Alloys. Compd. 793 (2019) 31–41.
[30] L. Zeng, H. Zeng, L. Jiang, et al., Anal. Chem. 91 (2019) 12070–12076.
[31] B. Huo, M. Du, A. Shen, et al., Anal. Chem. 91 (2019) 10979–10983.
[32] Y. Li, D. Jia, W. Ren, F. Shi, C. Liu, Adv. Funct. Mater. 29 (2019)1903191.
[33] Y. Kim, Y.J. Jang, D. Lee, B.S. Kim, D.G. Churchill, Sens. Actuators B: Chem. 238 (2017) 145–149.
[34] X. Zhou, Y. Zeng, C. Liyan, X. Wu, J. Yoon, Angew. Chem. Int. Ed. 55 (2016) 4729–4733.
[35] Z. Lei, Y. Yang, J. Am. Chem. Soc. 136 (2014) 6594–6597.
[36] Y.J. Jang, K. Kim, O.G. Tsay, D.A. Atwood, D.G. Churchill, Chem. Rev. 115 (2015) PR1–PR76.
[37] B.L. Huo, M. Du, A. Shen, et al., Anal. Chem. 91 (2019) 10979–10983.
[38] L. Chen, D. Wu, J. Yoon, ACS Sens. 3 (2018) 27–43.
[39] X. Sun, T.D. James, Chem. Rev. 115 (2015) 8001–8037.
[40] L. You, D. Zha, E.V. Anslyn, Chem. Rev. 115 (2015) 7840–7892.
[41] X. Zhou, S. Lee, Z. Xu, J. Yoon, Chem. Rev. 115 (2015) 7944–8000.
[42] S.K. Sheet, B. Sen, S. Khatua, Inorg. Chem. 58 (2019) 3635–3645.
[43] W. Wu, J. Dong, X. Wang, et al., Analyst 137 (2012) 3224–3226.
[44] S. Huang, Y. Wu, F. Zeng, L. Sun, S. Wu, J. Mater. Chem. C 4 (2016) 10105–10110.
[45] Y.C. Cai, C. Li, Q.H. Song, J. Mater. Chem. C 5 (2017) 7337–7343.
[46] T.J. Dale, J. Rebek Jr., Angew. Chem. Int. Ed. 48 (2009) 7850–7852.
[47] T.H. Ma, M. Dong, M. Dong, Y.W. Wang, Y. Peng, Chem. Eur. J. 16 (2010) 10313–10318.
[48] Y.M. Dong, Y. Peng, M. Dong, Y.W. Wang, J. Org. Chem. 76 (2011) 6962–6966.
[49] M. Dong, Y. Peng, M. Dong, N. Tang, Y.W. Wang, Org. Lett. 14 (2012) 130–133.
[50] M. Dong, Y.W. Wang, A.J. Zhang, Y. Peng, Chem. Asian J. 8 (2013) 1321–1330.
[51] Y.W. Wang, S.B. Liu, W.J. Ling, Y. Peng, Chem. Commun. 52 (2016) 827–830.
[52] Y.X. Hua, Y. Shao, Y.W. Wang, Y. Peng, J. Org. Chem. 82 (2017) 6259–6267.
[53] M.S.J. Khan, Y.W. Wang, M.O. Senge, Y. Peng, J. Hazard. Mater. 342 (2018) 10–19.
[54] S.S. Ali, A. Gangopadhyay, A.K. Pramanik, et al., Analyst 143 (2018) 4171–4179.
[55] T.I. Kim, S.B. Maity, J. Bouffard, Y. Kim, Anal. Chem. 88 (2016) 9259–9263.
[56] J. Yao, Y. Fu, W. Xu, et al., Anal. Chem. 88 (2016) 2497–2501.
[57] S. Gharami, K. Aich, S. Das, L. Patra, T.K. Mondal, New J. Chem. 43 (2019) 8627–8633.
[58] Y.C. Cai, C. Li, Q.H. Song, ACS Sens. 2 (2017) 834–841.
[59] M.R. Sambrook, S. Notman, Chem. Soc. Rev. 42 (2013) 9251–9267.
[60] Y.Q. Sun, M. Chen, J. Liu, et al., Chem. Commun. 47 (2011) 11029–11031.
[61] W.H. Melhuish, J. Phys. Chem. 65 (1961) 229–235.
[62] D. Lee, G. Kim, J. Yin, J. Yoon, Chem. Commun. 51 (2015) 6518–6520.
[63] CCDC 1962385 (FD1), 1962386 (FD2), and 1962387 (FD3) contain the supplementary crystallographic data for this paper. These data are provided free of charge by The Cambridge Crystallographic Data Centre.